

Near-Optimal Budgeted Data Exchange for Distributed Loop Closure Detection

Yulun Tian*, Kasra Khosoussi*, Matthew Giamou†, Jonathan P. How* and Jonathan Kelly†

*Laboratory for Information and Decision Systems (LIDS)

Massachusetts Institute of Technology

Email: {yulun,kasra,jhow}@mit.edu

†Space & Terrestrial Autonomous Robotic Systems (STARS) Laboratory

University of Toronto Institute for Aerospace Studies (UTIAS)

Email: {matthew.giamou,jonathan.kelly}@robotics.utias.utoronto.ca

Abstract—Inter-robot loop closure detection is a core problem in collaborative SLAM (CSLAM). Establishing inter-robot loop closures is a resource-demanding process, during which robots must consume a substantial amount of mission-critical resources (e.g., battery and bandwidth) to exchange sensory data. However, even with the most resource-efficient techniques, the resources available onboard may be insufficient for verifying every potential loop closure. This work addresses this critical challenge by proposing a resource-adaptive framework for distributed loop closure detection. We seek to maximize task-oriented objectives subject to a budget constraint on total data transmission. This problem is in general NP-hard. We approach this problem from different perspectives and leverage existing results on monotone submodular maximization to provide efficient approximation algorithms with performance guarantees. The proposed approach is extensively evaluated using the KITTI odometry benchmark dataset and synthetic Manhattan-like datasets.

I. INTRODUCTION

Multirobot systems can provide solutions to complex large-scale tasks that are otherwise beyond the capability of a single robot. Collaborative Simultaneous Localization and Mapping (CSLAM) is an indispensable part of any multirobot system requiring robots to navigate in an unknown GPS-denied environment; see [34] for a recent survey. Inter-robot loop closures lie at the heart of CSLAM: they tie individual trajectories and maps together, and allow spatial information to flow from one robot to the entire team. As a result, the success of CSLAM—and, consequently, that of the mission—is directly dependent upon detection of informative inter-robot loop closures.

Mobile robots are necessarily constrained by the limited resources they can carry on-board (e.g., batteries, processing power, wireless radios). These resources are especially scarce in the case of cost-effective multirobot systems. Addressing these limitations is a critical challenge in CSLAM. In particular, detecting inter-robot loop closures is a resource-demanding task [6–8,12,34] since robots must consume substantial amounts of energy and bandwidth to exchange their observations. This challenge has been recognized in numerous recent publications and has sparked a growing interest in designing *resource-efficient* frameworks that aim to minimize resource consumption due to data exchange in CSLAM front-ends [5–7,12,23]. However, even with the most resource-efficient data exchange policies [6–8,12], the available bandwidth and/or the allocated budget on energy consumption may still be insufficient for verifying all *potential* inter-robot loop closures. It is thus crucial for robots to be

able to seamlessly *adapt* to the allocated resource budgets by selecting a budget-feasible subset of potential loop closures.

We propose a *resource-adaptive* framework that aims to maximize task-oriented monotone submodular objectives subject to a budget constraint on data transmission in CSLAM front-ends. Giamou et al. [12] have recently shown that the minimum amount of data transmission required for verifying a given set of potential inter-robot loop closures is determined by the size of the minimum vertex cover in the corresponding *exchange graph*. This immediately implies that verifying the budget-feasibility of a proposed solution to our problem is basically equivalent to solving the vertex cover problem and thus is NP-complete in general. Furthermore, in this setting, the greedy measurement selection algorithms (i.e., selecting edges greedily) designed for standard cardinality constraints on the set of selected measurements [3,19,35] lack the necessary foresight and thus may exhaust their data transmission budgets rapidly, leading to arbitrarily poor performance.

Despite these challenges, after a change of variables and by establishing an approximation factor preserving reduction, we show that the natural greedy algorithm can still provide constant-factor approximation guarantees. The performance of the proposed approach is extensively validated using both real-world and simulated datasets. In particular, empirical near-optimality is demonstrated by leveraging natural convex relaxations. Ultimately, our work enables rendezvousing robots to collaboratively search for inter-robot loop closures by exchanging a near-optimal subset of their observations without exceeding an allocated data transmission budget.

An extended version of this paper containing the pseudocode and all proofs can be found in [37].

Notation. Bold lower-case and upper-case letters are reserved for vectors and matrices, respectively. $\mathbf{A} \succeq \mathbf{0}$ (resp., $\mathbf{A} \succ \mathbf{0}$) means that \mathbf{A} is positive semidefinite (resp., positive definite). $\mathcal{C}_w(\mathcal{E})$ denotes the minimum weighted vertex cover of the graph induced by the edge set \mathcal{E} where vertices are weighted by a positive weight function w . Finally, the value of $\mathcal{C}_w(\mathcal{E})$ is denoted by $c_w(\mathcal{E}) \triangleq \sum_{v \in \mathcal{C}_w(\mathcal{E})} w(v)$.

II. RELATED WORK

This paper focuses on CSLAM front-ends; see, e.g., [5,29,34] and references therein for state-of-the-art resource-efficient

CSLAM back-ends. We limit our discussion to prior works that either propose resource-aware CSLAM front-ends or use methods similar to ours on related problems.

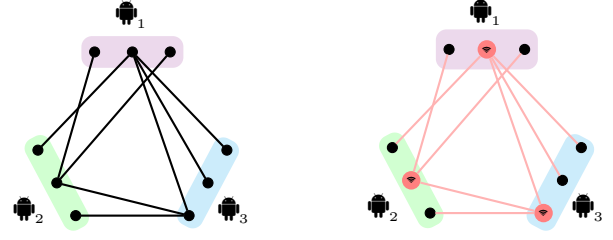
Choudhary et al. [5] circumvent the resource-intensive nature of data exchange in CSLAM front-ends by utilizing object models to reduce communication between robots, effectively compressing sensory observations with high-level semantic labels. Needless to say, their approach is limited to environments filled with known objects.

Cieslewski and Scaramuzza [6, 7] focus on designing data-efficient and scalable schemes for the “online query” phase of distributed place recognition. During this phase, robots exchange compact representations of their observations in order to decide to whom to send a full place query. The proposed methods reduce the amount of data transmission in this phase from $O(n^2)$ to $O(n)$ where n is the number of robots. It is empirically shown that the applied heuristics only incur a small loss in place recognition recall. We, however, focus on resource consumption due to exchanging *full* observations that takes place *after* this initial phase. As a result, our resource-adaptive framework can be used alongside [6–8] to improve the overall resource-efficiency of the system.

Once the query phase is complete, robots need to exchange full image keypoints for geometric verification and relative pose estimation. Giamou et al. [12] focus on resource-optimal exchange policies for this stage. The proposed problem formulation takes into account both the total amount of exchanged data and the induced division of labor among robots. The authors show that in the pairwise case, this problem is essentially equivalent to the minimum bipartite vertex cover problem and hence can be solved efficiently. Our paper is similar to [12] in that we also consider the more communication-intensive phase of full data exchange. However, our approach also explicitly considers the “value” of (e.g., information gained by) sharing each observation, and is able to deal with hard communication budgets.

Belief pruning and graph sparsification constitute another line of research in resource-efficient SLAM [14, 21, 31, 41]. In particular, Paull et al. [31] consider CSLAM in underwater environments where acoustic communication is high-latency, low-bandwidth, and unreliable. A consistent sparsification scheme is proposed in [31] to reduce the amount of transmitted data after marginalizing out variables. In [32], the authors further look at the combined problem of variable selection and graph sparsification, and propose a unified framework that takes into account computation, communication, and memory budgets. In this paper, we also cast our problem in a similar resource-adaptive setting. Unlike [32], however, we focus on the complementary problem of inter-robot loop closure detection in CSLAM front-ends.

Khosoussi et al. [18, 19] and Carlone and Karaman [3] have proposed measurement selection schemes for SLAM and visual-inertial navigation (VIN). In both applications, a cardinality constraint is imposed on the selected measurements to control the computational cost of solving the underlying estimation problem. In [18, 19], the authors use weighted tree-



(a) Example exchange graph (b) A lossless exchange policy

Fig. 1: (a) An example exchange graph \mathcal{G}_x in a 3-rendezvous where each robot owns three vertices (observations). To verify a potential inter-robot loop closure between two connected vertices, at least one robot needs to share its observation with the other robot. (b) A lossless exchange policy in which the observations associated to the vertices marked in red are transmitted. In the optimal exchange policy, robots must exchange 3 observations to cover all potential loop closures. Now if robots are only permitted to exchange at most $b = 2$ observations, they must decide which budget-feasible subset of potential loop closures is most valuable (in expectation) based a task-oriented objective.

connectivity [17] as a graphical surrogate for the D-optimality criterion to select high quality measurements. Similarly, in the context of VIN, Carlone and Karaman [3] use the D-optimality and E-optimality criteria to select a “valuable” subset of visual features for localization. Both of these approaches [3, 18, 19] leverage the monotone submodular property of the D-criterion to provide performance guarantees. In this paper, we also use the objective functions introduced in [3, 18, 19], albeit for *communication-constrained* scenarios.

III. PROBLEM FORMULATION:

OPT. RESOURCE-ADAPTIVE LOOP CLOSURE DETECTION

We begin by reviewing the general structure of decentralized inter-robot loop closure detection schemes [6, 7, 12]. CSLAM, by definition, relies on communication. Although maintaining a fully connected communication network may not be feasible at all times, robots must be able to at least occasionally communicate with some of their peers during close encounters—preplanned or otherwise. The inter-robot loop closure detection process occurs during a *rendezvous*.

Definition 1 (Rendezvous). An n -rendezvous ($n \geq 2$) refers to the situation where n robots are positioned such that each of them will receive the data broadcasted by any other robot in that group owing to the broadcast nature of wireless medium.

A. Metadata Exchange

Each robot arrives at a rendezvous with its own unique collection of observations (e.g., images or laser scans) acquired throughout its mission. Robots then exchange a *compact representation* of their observations (“metadata” according to [12]) in order to identify *potential* loop closures. Several choices are bag-of-words vectors [7, 12], low-dimensional feature vectors computed by a deep neural network [6], and/or spatial clues (i.e., estimated location with uncertainty) if robots have already established a common reference frame [12]. Comparing

metadata reveals a number of potential matches. Each potential match comes with a similarity score [10] or an *occurrence probability* (estimated directly or obtained by normalizing the similarity scores) that estimates the likelihood of that potential match corresponding to a true loop closure. The result can be naturally represented as an *exchange graph* [12].

Definition 2 (Exchange Graph). An exchange graph [12] is a simple undirected graph $\mathcal{G}_x = (\mathcal{V}_x, \mathcal{E}_x)$ where each vertex $v \in \mathcal{V}_x$ corresponds to an observation, and each edge $\{u, v\} \in \mathcal{E}_x$ corresponds to a potential inter-robot loop closure between the corresponding observations. Furthermore, \mathcal{G}_x is endowed with $w : \mathcal{V}_x \rightarrow \mathbb{R}_{>0}$ and $p : \mathcal{E}_x \rightarrow (0, 1]$ that quantify the size of each observation,¹ and the occurrence probability of an edge, respectively. We make the simplifying assumption that edges occur independently.

Note that in an n -rendezvous, the exchange graph will be an n -partite graph. Figure 1a illustrates a simple exchange graph with $n = 3$. For simplicity, we assume that a single robot participating the rendezvous (known as the “broker” in [12]) is responsible for forming the exchange graph and solving the subsequent optimization problem introduced in Section III-C. A fully decentralized approach is left for future work.

B. Optimal Lossless Data Exchange

After identifying potential matches, robots must exchange full observations for geometric verification and relative pose estimation [12]. This stage is substantially more communication-intensive than the metadata exchange phase as it involves the transmission of actual observations (e.g., the complete set of keypoints in an image). In [6, 7], each robot sends its full query *only* to the owner of the “most promising” potential match. This heuristic obviously comes at the risk of losing some loop closures.

Our recent work [12] presents an efficient algorithm for finding the optimal data exchange policy that minimizes data transmission among all *lossless* (i.e., allows robots to verify *every* potential match) exchange policies in 2-rendezvous. In [12] we demonstrate that by forming the exchange graph and exploiting its unique structure one can come up with intelligent resource-efficient data exchange policies which were not possible in [6, 7]. In particular, for 2-rendezvous we prove that in the optimal exchange policy, agents share the observations that correspond to the minimum weighted vertex cover of the exchange graph, $\mathcal{C}_w(\mathcal{E}_x) \subset \mathcal{V}_x$ [12]. Thus, the minimum amount of data transmission required for verifying all potential matches is given by $c_w(\mathcal{E}_x) \triangleq \sum_{v \in \mathcal{C}_w(\mathcal{E}_x)} w(v)$.

Here we note that this result can be trivially generalized to the case of n -rendezvous. Figure 1b illustrates an example. The key difference between 2-rendezvous and n -rendezvous is that finding the optimal lossless exchange policy (i.e., the minimum weighted vertex cover) is NP-hard for general n -rendezvous (i.e., general n -partite graphs) when $n \geq 3$. Nevertheless, by rounding the solution of linear programming (LP) relaxation

we obtain a lossless exchange policy with at most $2c_w(\mathcal{E}_x)$ data transmission [40].

C. Data Exchange under Budgeted Communication

Intrinsic limitations of the communication channel (e.g., bandwidth in underwater acoustic communication [31]), operational constraints, and/or resource scheduling policies (e.g., enforced to regulate resource consumption) necessitate and lead to budgeted communication. We are specifically interested in situations where the data transmission budget b is strictly less than $c_w(\mathcal{E}_x)$. Based on our earlier remarks, one can immediately conclude that in this regime, verifying all potential matches without exceeding the budget b becomes impossible. Therefore, resource-adaptation and task-oriented prioritization are inevitable. In what follows, we approach this problem from two perspectives. It will become clear shortly that these two seemingly different viewpoints lead to two problem statements that are intimately connected.

1) *Edge Selection*: From the perspective of measurement selection [3, 18, 19], we seek to select a subset of potential loop closures such that the minimum amount of data transmission needed to verify them is at most b . We need a task-oriented objective $f_e : 2^{\mathcal{E}_x} \rightarrow \mathbb{R}_{\geq 0}$ that quantifies the value of all subsets of potential loop closures. Note that f_e must take into account the stochastic nature of potential matches, captured by the edge weights $p : \mathcal{E}_x \rightarrow (0, 1]$ in \mathcal{G}_x . Later in this section we discuss several suitable choices of f_e for CSLAM and place recognition. This perspective leads to the following problem statement:

$$\underset{\mathcal{E} \subseteq \mathcal{E}_x}{\text{maximize}} \quad f_e(\mathcal{E}) \quad \text{s.t.} \quad c_w(\mathcal{E}) \leq b, \quad (\text{P}_e)$$

where $c_w(\mathcal{E})$ gives the minimum amount of data transmission needed to verify \mathcal{E} (see Section III-B) and $c_w(\mathcal{E}) \leq b$ imposes a global communication budget on the rendezvousing robots.

Remark 1. Merely deciding whether a given $\mathcal{E} \subseteq \mathcal{E}_x$ is P_e -feasible, (i.e., there exists a vertex cover for \mathcal{E} with a size of at most b), is an instance of the weighted vertex cover problem which is NP-complete [16] in n -rendezvous with $n \geq 3$. Put differently, deciding whether a set of potential loop closures can be verified by exchanging at most b units of data is NP-complete when $n \geq 3$.

2) *Vertex Selection*: From the perspective of data exchange policies, one may naturally search for an optimal subset of vertices (observations) that need to be broadcasted without exceeding the budget b . Recall that once an observation is broadcasted, other robots can collectively verify *all* potential loop closures involving that observation (i.e., incident to the selected vertex); see Figure 1 and [12]. This motivates the following objective function,

$$f_v : 2^{\mathcal{V}_x} \rightarrow \mathbb{R}_{\geq 0} : \mathcal{V} \mapsto f_e(\text{edges}(\mathcal{V})). \quad (1)$$

where $\text{edges} : 2^{\mathcal{V}_x} \rightarrow 2^{\mathcal{E}_x}$ gives the set of all edges such that for each edge at least one end is in the given subset of vertices. This intuitively means that the value of any subset of vertices

¹For instance, this can be the number of keypoints in an image.

is equal to the f_e -value of all edges incident to those vertices. This leads to the following optimization problem:

$$\underset{\mathcal{V} \subseteq \mathcal{V}_x}{\text{maximize}} f_v(\mathcal{V}) \quad \text{s.t.} \quad \sum_{v \in \mathcal{V}} w(v) \leq b, \quad (\text{P}_v)$$

Note that the budget constraint in P_v is simpler than what we encountered in P_e . Needless to say, P_e and P_v are closely related. The connection between these two problems is discussed and exploited in Section IV.

D. Objective Function

Definition 3. A set function $f : 2^{\mathcal{W}} \rightarrow \mathbb{R}_{\geq 0}$ for a finite \mathcal{W} is normalized, monotone, and submodular (NMS) if it satisfies the following properties:

- ◊ Normalized: $f(\emptyset) = 0$.
- ◊ Monotone: for any $\mathcal{A} \subseteq \mathcal{B}$, $f(\mathcal{A}) \leq f(\mathcal{B})$.
- ◊ Submodular: for any $\mathcal{A} \subseteq \mathcal{B}$ and $u \in \mathcal{W} \setminus \mathcal{B}$, $f(\mathcal{B} \cup \{u\}) - f(\mathcal{B}) \leq f(\mathcal{A} \cup \{u\}) - f(\mathcal{A})$.

We focus only on cases where f_e is NMS. In what follows, we briefly review two examples of such functions used recently for measurement selection in the context of SLAM and VIN [3, 18, 19]. In addition, we consider also a third objective that is suitable for general place recognition scenarios. Note that our framework is compatible with *any* NMS objectives, and is not limited to the instances considered below.

1) D-optimality Criterion

The D-optimality design criterion (D-criterion), defined as the log-determinant of the Fisher information matrix (FIM), is one of the most popular design criteria in the theory of optimal experimental design with well-known geometrical and information-theoretic interpretations; see, e.g., [15, 33]. D-criterion has been widely adopted in many problems including sensor selection [15, 35] and measurement selection in SLAM [3, 18]. Let $\mathbb{I}_{\text{init}} \succ \mathbf{0}$ denote the information matrix of the joint CSLAM problem before incorporating the potential loop closures. Moreover, let $\mathbb{I}_e = \mathbf{J}_e^\top \Sigma_e^{-1} \mathbf{J}_e \succeq \mathbf{0}$ be the information matrix associated to the candidate loop closure $e \in \mathcal{E}_x$ in which \mathbf{J}_e and Σ denote the measurement Jacobian matrix and the covariance of Gaussian noise, respectively. Following [3], one can approximate the expected gain in the D-criterion as:

$$f_{\text{FIM}}(\mathcal{E}) \triangleq \log \det \left(\mathbb{I}_{\text{init}} + \sum_{e \in \mathcal{E}} p(e) \cdot \mathbb{I}_e \right) - \log \det \mathbb{I}_{\text{init}}. \quad (2)$$

f_{FIM} is NMS [3, 35].

2) Tree-Connectivity

The D-criterion in 2D pose-graph SLAM can be closely approximated by the weighted number of spanning trees (WST)—hereafter, tree-connectivity—in the graphical representation of SLAM [17]. In [18, 19] tree-connectivity is used as a graphical surrogate for the D-criterion for (potential) loop closure selection. Evaluating tree-connectivity is computationally cheaper than evaluating the D-criterion and, furthermore, does not require any metric knowledge of robots' trajectories. Let $t_{w_p}(\mathcal{E})$ and $t_{w_\theta}(\mathcal{E})$ denote the

weighted number of spanning trees in a pose-graph specified by the edge set \mathcal{E} whose edges are weighted by the precision of the translational and rotational measurements, respectively [19]. Furthermore, let $\mathcal{E}_{\text{init}}$ be the set of edges that exist in the CSLAM pose-graph prior to the rendezvous. Define $\Phi(\mathcal{E}) \triangleq 2 \cdot \log \mathbb{E}[t_{w_p}(\mathcal{E}_{\text{init}} \cup \mathcal{E})] + \log \mathbb{E}[t_{w_\theta}(\mathcal{E}_{\text{init}} \cup \mathcal{E})]$ where expectation is with respect to the anisotropic random graph model defined in Definition 2; see [19]. Khosoussi et al. [19] then seek to maximize the following objective:

$$f_{\text{WST}}(\mathcal{E}) \triangleq \Phi(\mathcal{E}) - \Phi(\emptyset). \quad (3)$$

It is shown in [18, 19] that f_{WST} is NMS if the underlying pose-graph is connected prior to the rendezvous.

3) Expected Number of True Loop Closures

The previous two estimation-theoretic objective functions are well suited for CSLAM. However, in the context of distributed place recognition, one may simply wish to maximize the expected number of true loop closures (NLC) between the agents. From Definition 2 recall that the probability associated to a potential loop closure $e \in \mathcal{E}_x$ is $p(e)$. Consequently, the expected number of true loop closures in a subset of edges \mathcal{E} can be expressed as:

$$f_{\text{NLC}}(\mathcal{E}) \triangleq \begin{cases} \sum_{e \in \mathcal{E}} p(e) & \mathcal{E} \neq \emptyset, \\ 0 & \mathcal{E} = \emptyset. \end{cases} \quad (4)$$

f_{NLC} is clearly NMS.

IV. ALGORITHM AND THEORETICAL GUARANTEES

This section presents approximation algorithms for our two perspectives P_v and P_e with performance guarantees that hold for any NMS f_e and the corresponding f_v .

Theorem 1. For any NMS f_e , the corresponding f_v is NMS.

This theorem implies that P_v is an instance of the classical problem of maximizing an NMS function subject to a knapsack constraint. Although this class of problems generalizes the maximum coverage problem [13] and thus are NP-hard in general, they enjoy a rich body of results on constant-factor approximation algorithms [20].² We discuss these algorithms in more detail and show how they can be applied to P_v in Section IV-A.

Now, we show that by establishing a simple approximation factor preserving reduction from P_e to P_v , we can also obtain constant-factor approximation schemes for P_e . Let OPT_e and OPT_v be the optimal values of P_e and P_v , respectively. The following lemmas shed more light on the connection between our two perspectives P_e and P_v .

Lemma 1.

- 1) For any P_v -feasible \mathcal{V} , $\text{edges}(\mathcal{V})$ is P_e -feasible.
- 2) $\text{OPT}_e = \text{OPT}_v$.

²Recall that an α -approximation algorithm for a maximization problem is an efficient algorithm that produces solutions with a value of at least $\alpha \cdot \text{OPT}$ for a constant $\alpha \in (0, 1)$.

Using the above lemma, we establish the following approximation factor preserving reduction from P_e to P_v . It is worth mentioning this reduction belongs to a strong class known as “S-reductions” [2,9].

Theorem 2. Given an α -approximation algorithm for P_v , the following is an α -approximation algorithm for P_e :

- 1) Run the α -approximation algorithm on P_v to produce \tilde{V} .
- 2) Return $\text{edges}(\tilde{V})$.

Theorem 2 illustrates how constant-factor approximation algorithms for P_v can be used as a proxy to obtain constant-factor approximation algorithms for the dual perspective in P_e . In Section IV-A, we show how the interplay between P_v and P_e can be exploited in certain situations to further improve the approximation guarantees of our algorithms.

A. Approximation Algorithms

So far, we have shown that near-optimal solutions to P_v and—by virtue of Theorem 2— P_e can be obtained using constant-factor approximation algorithms for maximizing NMS functions under a knapsack constraint. Some of these algorithms are listed in Table I; see [20] for a comprehensive survey. The approximation factors obtained by these algorithms hold for any NMS objectives. In the special case of maximizing the expected number of loop closures f_{NLC} (Section III-D) under a cardinality constraint, P_v reduces to the well-studied maximum coverage problem over a graph [13]. In this case, a simple procedure based on pipage rounding can improve the approximation factor to $3/4$ [1]. Furthermore, if the graph is bipartite, a specialized algorithm can improve the approximation factor to $8/9$ [4]. Nonetheless, in this work we focus on greedy algorithms described in Table I due to their generality, computational efficiency, and incremental nature (see Remark 2).

In many real-world scenarios, the number of primitives (e.g., keypoints in an image) is roughly the same across all measurements. By ignoring insignificant variations in observations sizes, one can assume that each vertex (i.e., observation) has unit weight or size. In this case, the knapsack constraint in P_v reduces to a cardinality constraint $|\mathcal{V}| \leq b$. We first discuss this case and then revisit the more general case of knapsack constraints.

1) Uniform Observation Size: The standard greedy algorithm gives the optimal approximation factor for maximizing general NMS functions under a cardinality constraint (Table I). This algorithm, when applied on P_v under a cardinality constraint, is as follows: for b rounds, greedily pick (without replacement) a vertex v with the highest marginal gain $f_v(\mathcal{V} \cup \{v\}) - f_v(\mathcal{V})$, where \mathcal{V} denotes the current set of selected vertices. Refer to Algorithm 1 in the extended version of this paper for the complete pseudocode [37]. The solution \mathcal{V}_{grd} produced by the greedy algorithm satisfies $f_v(\mathcal{V}_{\text{grd}}) \geq (1 - 1/e) \cdot \text{OPT}_v$ [28]. Furthermore, by our approximation-factor-preserving reduction (Theorem 2), \mathcal{V}_{grd} can in turn be mapped to a P_e -feasible subset of edges $\mathcal{E}_{\text{grd}} = \text{edges}(\mathcal{V}_{\text{grd}})$, for which we also have $f_e(\mathcal{E}_{\text{grd}}) \geq (1 - 1/e) \cdot \text{OPT}_e$.

Remarkably, in some cases the interplay between P_e and P_v reveals a pathway to further improve the solution even after b rounds of standard greedy selection. We already know that \mathcal{E}_{grd} can be covered by a subset of vertices of size b , namely \mathcal{V}_{grd} . However, there may be an even “cheaper” (i.e., of size $b' < b$) subset of vertices that covers the entire \mathcal{E}_{grd} . Such a subset can be found by computing the minimum vertex cover of the graph induced by \mathcal{E}_{grd} . This is in general NP-hard. We can, however, find a vertex cover by rounding a solution of the LP relaxation of this problem; see [40]. For 2-rendezvous (bipartite exchange graphs), this gives the minimum vertex cover as noted in [12]. As mentioned earlier, for general n -rendezvous ($n \geq 3$), size of the resulting vertex cover is guaranteed to be at most twice the size of the minimum vertex cover; see, e.g., [40]. If such a subset can be found, we can continue running the greedy algorithm for $b - b'$ additional rounds while still ensuring that the final solution is budget-feasible. Suppose repeating the process of recomputing the (approximate) minimum vertex cover leads to $b + k$ rounds of greedy decisions in total and produces \mathcal{V}_{grd} . Using [20, Theorem 1.5], it can be shown that $f_v(\mathcal{V}_{\text{grd}}) \geq (1 - 1/e^{1+\frac{k}{b}}) \cdot \text{OPT}_v$. However, we must note that in practice, recomputing the vertex cover only tends to improve the solution when the input exchange graph is sufficiently dense, and in 2-rendezvous where the actual minimum vertex cover can be computed.

Remark 2. According to [30], an algorithm is “any-com” if it finds “a suboptimal solution quickly and refines it as communication permits”. The greedy algorithm described above has a similar trait: (i) for any budget b , it finds a near-optimal solution; (ii) let $(\mathcal{E}_{\text{grd}}^b, \mathcal{V}_{\text{grd}}^b)$ be the pair of near-optimal solutions produced for budget b . Then, $\mathcal{V}_{\text{grd}}^b$ must be sent as a priority queue to robots to initiate the data exchange process by following the original ordering prescribed by the greedy algorithm (i.e., first round, second round, etc). Now imagine the exchange process is interrupted after exchanging $b' < b$ observations. Due to the incremental nature of the greedy algorithm, at this point robots have already exchanged $\mathcal{V}_{\text{grd}}^{b'}$, which is the solution that would have been produced by the greedy algorithm if the budget was b' . But note that we know that this solution and its corresponding subset of loop closures $\mathcal{E}_{\text{grd}}^{b'}$ are near-optimal for budget b' .

2) Non-uniform Observation Size: A modified version of the greedy algorithm is guaranteed to provide a solution with an approximation factor of $1/2 \cdot (1 - 1/e)$ [20,24] (Table I) for the knapsack constraint. The algorithm is very intuitive: first, we run the standard greedy algorithm described above (stopping condition in this case will be the knapsack constraint). Then, we rerun the greedy algorithm with a minor modification: instead of picking the vertex with the highest marginal gain, we select the one with the highest *normalized* marginal gain, i.e., $(f_v(\mathcal{V} \cup \{v\}) - f_v(\mathcal{V})) / w(v)$. Finally, we return the better solution. Note that the normalized marginal gain encodes the marginal gain achieved in our task-oriented objective per one bit of data transmission. For example, for f_{NLC} (4) this term quantifies the expected number of realized loop closures

TABLE I: A summary of approximation algorithms for maximizing NMS functions based on [20]

Observation Size (Vertex Weight)	S-reduction to NMS Max. Under	Approximation Factor
Non-uniform	Knapsack constraint	Greedy* [24] $1/2 \cdot (1 - 1/e)$ AND $1 - 1/e$ [36]
Uniform	Cardinality constraint	Standard Greedy $1 - 1/e$ [28]

gained by broadcasting $v \in \mathcal{V}_x$ per unit of transmitted data.

B. Computational Complexity Under Uniform Weights

The standard greedy algorithm needs $O(b \cdot m)$ evaluations of f_v where m denotes the number of vertices in the exchange graph (e.g., number of images among which the search for inter-robot loop closures takes place). Note that in practice $m \geq n$ depends on the number of rendezvousing robots n . The number of function calls can be reduced using the so-called lazy greedy method [20,26]. Evaluating f_{NLC} takes $O(1)$ time. By contrast, evaluating f_{WST} and f_{FIM} can be quite costly as they both require computing log-determinant of matrices of size $O(d)$ where d denotes the number robot poses in the global pose-graph. For dense pose-graphs, a naïve implementation runs in $O(b \cdot m \cdot d^3)$ time. A more clever implementation [18,19] can reduce this to $O(b \cdot d^3 + b \cdot m \cdot d^2)$, or even $O(d^3 + b \cdot m \cdot d^2)$. Leveraging the sparse structure of real-world pose-graphs eliminates the cubic dependence of run time on d . In addition, the greedy algorithm enjoys an “embarrassingly parallel” structure that can be easily exploited to significantly speed up the task of screening candidates and thus reduce the impact of m on the run time.

C. Certifying Near-Optimality via Convex Relaxation

Evaluating the performance of the proposed approximation algorithms for a particular instance of our problem requires the value of OPT. Computing OPT by brute force is impractical even in rather small scenarios. Given an upper bound $\text{UPT} \geq \text{OPT}$, one can compare the value attained by an approximation algorithm with UPT as a surrogate for OPT. Therefore, UPT provides an *a posteriori* certificate for near-optimality of \mathcal{V}_{grd} .

We obtain such a certificate by first formulating our combinatorial optimization problem as an integer program (similar to the standard integer linear programming formulation of the maximum coverage problem), and then computing the optimal value of its natural convex relaxation. Consider indicator variables $\pi \triangleq [\pi_1, \dots, \pi_n]^\top$ and $\ell \triangleq [\ell_1, \dots, \ell_m]^\top$ where each π_i corresponds to a vertex (similar to [12]; see Section III) and each ℓ_i corresponds to an edge in the exchange graph. Let \mathbf{A} be the (undirected) incidence matrix of the exchange graph and \mathbf{w} be the stacked vector of vertex weights. Define $\mathcal{F}_{\text{int}} \triangleq \{(\pi, \ell) \in \{0,1\}^n \times \{0,1\}^m : \mathbf{w}^\top \pi \leq b, \mathbf{A}^\top \pi \geq \ell\}$. The objective functions introduced in Section III can all be expressed in terms of indicator variables ℓ . For example, the D-criterion (2) can be expressed as $h(\ell) \triangleq \log \det(\mathbb{I}_{\text{init}} + \sum_{e \in \mathcal{E}_{\text{all}}} \ell_e \cdot p(e) \cdot \mathbb{I}_e)$; see also [3,18]. It is easy to observe that maximizing $h(\ell)$ subject to $(\pi, \ell) \in \mathcal{F}_{\text{int}}$ is equivalent to \mathbf{P}_e with the corresponding objective function. Now relaxing \mathcal{F}_{int} to $\mathcal{F} \triangleq \{(\pi, \ell) \in [0,1]^n \times [0,1]^m : \mathbf{w}^\top \pi \leq b, \mathbf{A}^\top \pi \geq \ell\}$ results in convex optimization problems for each of the objective

functions introduced in Section III (an LP for f_{NLC} and max-det problems [39] subject to additional affine constraints for f_{WST} and f_{FIM}). This upper bound is used in Section V to certify the near-optimality of the solutions produced by the greedy algorithms. These problem instance-specific certificates are often much stronger than our theoretical worst-case guarantees.

V. EXPERIMENTS

In this section, we demonstrate the main features of our proposed approach with both simulated and real-world datasets. In our experiments, all pose-graph SLAM instances are solved using g2o [22]. All convex relaxation problems introduced in Section IV-C are modeled using the YALMIP toolbox [25] and solved using SDPT3 [38] in MATLAB.

A. General Setup

A key property of our proposed approach is its compatibility with any task-oriented NMS objective function. In our experiments, we consider the three functions introduced in Section III-D: (i) D-optimality criterion (FIM); (ii) weighted tree-connectivity (WST), and (iii) expected number of loop closures (NLC). Our main goal is not to compare these objective functions, but to highlight the general applicability of our approach and evaluate it with standard task-oriented metrics. Still, we point out that in practice, different objectives lead to different computation and communication overhead in the metadata exchange phase. As discussed in Section IV-B, f_{FIM} and f_{WST} incur more computation overhead than f_{NLC} , as evaluating them requires computing the log-determinant of large matrices. In terms of communication, f_{FIM} incurs the highest overhead. f_{WST} incurs less communication overhead than f_{FIM} , as it only requires the structure of the pose-graph [19]. Finally, f_{NLC} incurs no communication overhead.

In this work, we do not impose a communication budget on the metadata exchange phase. This is done for two reasons. First, in the place recognition pipeline introduced in Section III, metadata exchange only constitutes a small fraction of the overall resource consumption. Second, the overhead that arises in the metadata exchange phase is objective-dependent in nature. Thus, counting the overhead as part of the resource consumption introduces unnecessary bias towards certain objectives (e.g., f_{NLC}). Nevertheless, we note that the proposed framework can be trivially extended to account for additional resource consumption beyond the main data exchange phase.

We introduce two algorithms as baselines. One natural way to approach Problem \mathbf{P}_e is to greedily select edges \mathcal{E} from \mathcal{E}_x until violating the vertex cover constraint $c_w(\mathcal{E}) \leq b$. In what follows, we call this baseline algorithm “Edge Greedy”. Note that Edge Greedy is a computationally expensive procedure,

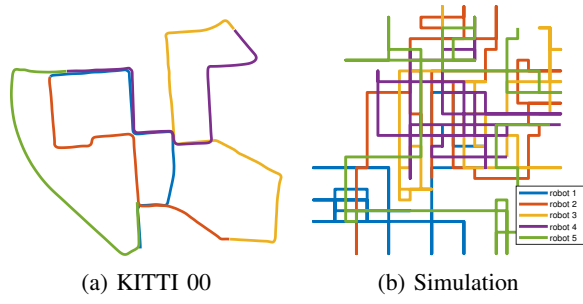


Fig. 2: Left: KITTI 00; Right: 2D simulation. Each base graph shows trajectories of five robots. Before inter-robot data exchange, trajectories are estimated purely using prior beliefs and odometry measurements, hence the drift displayed in the KITTI trajectories. The simulation trajectories shown are the exact ground truth.

as it requires (approximately) solving the minimum vertex cover problem multiple times during the greedy loop. In our implementation, we further augment Edge Greedy by allowing it to select extra “communication free” edges, i.e., edges that are incident to the current vertex cover. Our second baseline is a simple random algorithm, which picks a random budget-feasible subset of observations and selects all potential loop closures that can be verified by sending these observations.

When comparing different algorithms, performance is evaluated in terms of the normalized objective value, i.e. achieved objective value divided by the maximum achievable value given infinite budget (i.e., selecting all candidates in \mathcal{E}_x). A crucial step is to demonstrate and verify the near-optimal performance of the proposed algorithm. Since finding the optimal value of Problem P_e is impractical, we rely on the proposed convex relaxation approach (Section IV-C) as an *a posteriori* certificate of near-optimality. In addition, to quantify how much accuracy we lose by using only a subset of loop closures, we compute the absolute trajectory error (ATE) between our estimated trajectory and the full maximum likelihood estimate (obtained by selecting all candidate loop closures).

B. KITTI Odometry Sequence 00

In order to show that the proposed algorithms are useful in real-world scenarios, we performed a number of offline experiments on data from the KITTI odometry benchmark [11]. Similar to [8], we divide the odometry sequence 00 into sub-trajectories representing individual robots’ paths (Figure 2a). This particular sequence contains many realistic path intersections and re-traversals, providing a large number of inter-robot loop closures that make the measurement selection problem interesting. For the KITTI experiments, we use a modified version of ORB-SLAM2 [27] to generate stereo visual odometry and potential loop closures. As in [12], we define the probability associated with each potential loop closure by normalizing the corresponding visual similarity score outputted by DBoW2 [10]. Since the weighted tree-connectivity (WST) objective only supports 2D data, we project the KITTI data to the x - y plane and work with the projected 2D trajectories. The same projection is done for the other two objective functions to ensure a fair comparison.

In practice, the number of keypoints is roughly the same (around 2000) for all observations obtained by ORB-SLAM2. In our experiments, we ignore this insignificant variation in observation sizes and assign each vertex a unit weight. In this way, our communication budget reduces to a cardinality constraint on the total number of observations the team can exchange. Assuming each keypoint (consisting of a descriptor and coordinates) uses approximately 40 bytes of data, a communication budget of 50, for example, translates to 4MB of total data exchange bandwidth.

Figures 3a-3c illustrate the performance of the proposed algorithm under different objective functions and varying communication budget. Under all three objectives, the proposed algorithm outperforms both baselines by a significant margin. Intuitively, the Edge Greedy baseline blindly maximizes the objective function without controlling resource consumption, while the random baseline only aims at achieving a budget-feasible solution. In contrast, by having foresight over resource consumption while maximizing the objective, the proposed method spends the budget more wisely, hence always achieving a higher score. Furthermore, Figures 3b (WST) and 3c (NLC) show upper bounds on the value of the optimal solution obtained using convex relaxation (Section IV-C). We do not include the upper bound for the FIM objective because solving the convex relaxation in this case is too time consuming.³ For both WST and NLC objectives, we observe that the performance of the proposed algorithm is close to the convex relaxation upper bound. This confirms our intuition that in practice, the proposed algorithm performs much better than the theoretical lower bound of $(1 - 1/e) \cdot \text{OPT}_e$. It is particularly interesting that for the NLC objective, the value achieved by the proposed approach matches exactly with the upper bound, indicating that in this case the solution is actually optimal. This happens because the specific problem instance is sparse, i.e., candidate edges form several distinct connected components. In this case, the entire problem breaks down into multiple easier sub-problems, for which it is more likely for the greedy algorithm to obtain an optimal solution. Due to the same sparse structure, we do not observe improvement caused by recomputing the minimum vertex cover, as discussed in Section IV-A.

Figure 3d illustrates the cross-objective performance of the proposed method evaluated on the absolute trajectory error (ATE). We note that the overall decrease in error is small as communication budget increases. This suggests that our initial estimate is relatively accurate. Nevertheless, as the communication budget increases, the estimates of all three objectives eventually approach the full maximum likelihood estimate (obtained by selecting all potential loop closures). Interestingly, the ATE metric is not monotonically decreasing. Furthermore, the performance of the NLC objective is more stable compared to the FIM and WST objectives. Both observations are due to the fact that the ATE is highly

³The KITTI dataset we use contains more than 2000 poses in total. Consequently, the Fisher information matrix with three degrees of freedom has dimension larger than 6000×6000 .

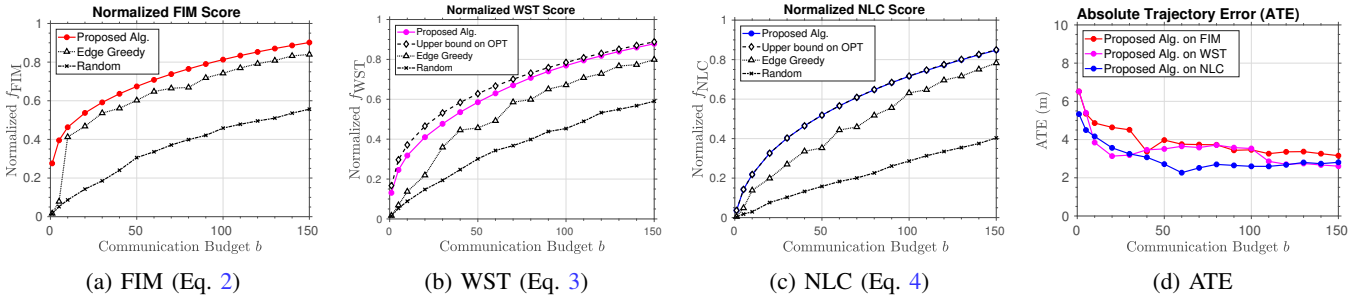


Fig. 3: (a) to (c) shows performance of the proposed algorithm in KITTI 00 under different objective functions and varying communication budget. Objective value is normalized by the maximum achievable value of each objective given infinite budget (selecting all potential loop closures). (d): cross-objective performance evaluated on ATE, compared against the maximum likelihood estimate given infinite budget. In the KITTI experiments, budget b is defined as the total number of observations the team can exchange. In this dataset, the minimum budget to cover all potential loop closures is 250, which translate to roughly 20MB of total data exchange bandwidth.

dependent on the random realization of the selected loop closures. Intuitively, although the FIM and WST objectives tend to select more informative loop closure candidates, these candidates may turn out to be false positives and hence do not contribute to the final localization accuracy. From this perspective, the NLC objective is advantageous as it seeks to maximize the expected number of true loop closures. However, the other two objectives can be easily augmented to better cope with the stochastic nature of candidate loop closures. This can be done by, e.g., prefiltering the candidates and removing those with low occurrence probabilities.

C. Simulation Experiments

Synthetic data was produced using the 2D simulator functionality of g2o [22]. The simulator produced noisy odometry and loop closure constraints for robots moving in a random square grid pattern (Figure 2b). The trajectory was divided into multiple robots in the same manner as the KITTI data, but loop closures probabilities p were generated from a uniform random distribution. We use a simulated graph to study the behavior of the proposed algorithm under varying densities of the input exchange graph. In our simulation, we control this density by enforcing different maximum degrees on the vertices and randomly pruning excess candidate edges. Figure 4 displays the effect of increasing density (in terms of the maximum vertex degree) on the WST objective. The algorithms were applied with a fixed communication budget of 50 over the same exchange graph. As expected, the proposed algorithm outperforms the baselines by a significant margin.

VI. CONCLUSION & FUTURE WORK

Inter-robot loop closures constitute the essence of collaborative localization and mapping; without them “collaboration” is impossible. Detecting inter-robot loop closures is a resource-intensive process, during which robots must exchange substantial amounts of sensory data. Recent works have made great strides in making CSLAM front-ends more data efficient [8,12]. While such approaches play a crucial role in saving scarce mission-critical resources, in many scenarios the resources available onboard (mainly, battery and bandwidth) may be insufficient for verifying every potential loop closure.

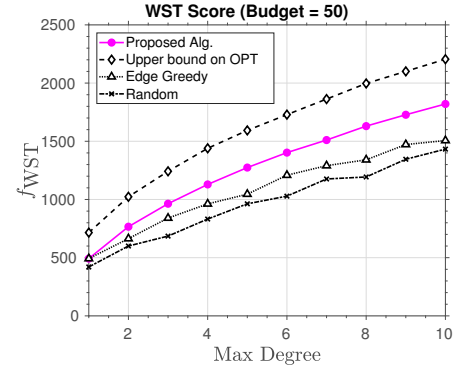


Fig. 4: Performance of the proposed algorithm maximizing the WST objective in simulation under fixed communication budget (50 in this case) and varying maximum degree of the exchange graph.

Consequently, robots must be able to solve the inter-robot loop closure detection problem under budgeted communication.

This paper addressed this critical challenge by adopting a resource-adaptive approach. In particular, we presented “any-com” constant-factor approximation algorithms for the problem of selecting a budget-feasible subset of potential loop closures while maximizing a task-oriented objective. Performance guarantees presented in this work hold for any monotone submodular objective. Extensive experimental results using the KITTI benchmark dataset and realistic synthetic data validated our theoretical results.

We plan to extend our results by considering new forms of communications constraints. In particular, in heterogeneous multirobot systems, one may wish to partition the team into several disjoint blocks and impose different communication budgets on each block. Our preliminary results indicate that our approach can be extended to cover this case. While beyond the scope of this paper, analyzing more complex communication protocols and network topologies is another important future direction.

ACKNOWLEDGEMENT

This work was supported in part by the NASA Convergent Aeronautics Solutions project Design Environment for Novel Vertical Lift Vehicles (DELIVER), by the Northrop Grumman Corporation, and by ONR under BRC award N000141712072.

REFERENCES

- [1] Alexander A. Ageev and Maxim I. Sviridenko. Approximation algorithms for maximum coverage and max cut with given sizes of parts. In Gérard Cornuéjols, Rainer E. Burkard, and Gerhard J. Woeginger, editors, *Integer Programming and Combinatorial Optimization*, pages 17–30, Berlin, Heidelberg, 1999. Springer Berlin Heidelberg. ISBN 978-3-540-48777-7.
- [2] Giorgio Ausiello, Pierluigi Crescenzi, Giorgio Gambosi, Viggo Kann, Alberto Marchetti-Spaccamela, and Marco Protasi. *Complexity and approximation: Combinatorial optimization problems and their approximability properties*. Springer Science & Business Media, 2012.
- [3] Luca Carlone and Sertac Karaman. Attention and anticipation in fast visual-inertial navigation. In *Robotics and Automation (ICRA), 2017 IEEE International Conference on*, pages 3886–3893. IEEE, 2017.
- [4] Bugra Caskurlu, Vahan Mkrtchyan, Ojas Parekh, and K. Subramani. On partial vertex cover and budgeted maximum coverage problems in bipartite graphs. In Josep Diaz, Ivan Lanese, and Davide Sangiorgi, editors, *Theoretical Computer Science*, pages 13–26, Berlin, Heidelberg, 2014. Springer Berlin Heidelberg.
- [5] Siddharth Choudhary, Luca Carlone, Carlos Nieto, John Rogers, Henrik I Christensen, and Frank Dellaert. Distributed mapping with privacy and communication constraints: Lightweight algorithms and object-based models. *The International Journal of Robotics Research*, 36(12):1286–1311, 2017. doi: 10.1177/0278364917732640.
- [6] Titus Cieslewski and Davide Scaramuzza. Efficient decentralized visual place recognition from full-image descriptors. In *1st International Symposium on Multi-Robot and Multi-Agent Systems*, 2017.
- [7] Titus Cieslewski and Davide Scaramuzza. Efficient decentralized visual place recognition using a distributed inverted index. *IEEE Robotics and Automation Letters*, 2(2):640–647, 2017.
- [8] Titus Cieslewski, Siddharth Choudhary, and Davide Scaramuzza. Data-efficient decentralized visual SLAM. *CoRR*, abs/1710.05772, 2017. URL <http://arxiv.org/abs/1710.05772>.
- [9] Pierluigi Crescenzi. A short guide to approximation preserving reductions. In *Computational Complexity, 1997. Proceedings., Twelfth Annual IEEE Conference on (Formerly: Structure in Complexity Theory Conference)*, pages 262–273. IEEE, 1997.
- [10] Dorian Gálvez-López and J. D. Tardós. Bags of binary words for fast place recognition in image sequences. *IEEE Transactions on Robotics*, 28(5):1188–1197, October 2012. ISSN 1552-3098. doi: 10.1109/TRO.2012.2197158.
- [11] Andreas Geiger, Philip Lenz, and Raquel Urtasun. Are we ready for autonomous driving? the kitti vision benchmark suite. In *Conference on Computer Vision and Pattern Recognition (CVPR)*, 2012.
- [12] Matthew Giamou, Kasra Khosoussi, and Jonathan P How. Talk resource-efficiently to me: Optimal communication planning for distributed loop closure detection. In *IEEE International Conference on Robotics and Automation (ICRA)*, 2018.
- [13] Dorit S Hochbaum. *Approximation algorithms for NP-hard problems*. PWS Publishing Co., 1996.
- [14] G. Huang, M. Kaess, and J. J. Leonard. Consistent sparsification for graph optimization. In *2013 European Conference on Mobile Robots*, pages 150–157, Sept 2013. doi: 10.1109/ECMR.2013.6698835.
- [15] Siddharth Joshi and Stephen Boyd. Sensor selection via convex optimization. *Signal Processing, IEEE Transactions on*, 57(2):451–462, 2009.
- [16] Richard M Karp. Reducibility among combinatorial problems. In *Complexity of computer computations*, pages 85–103. Springer, 1972.
- [17] Kasra Khosoussi, Shoudong Huang, and Gamini Dissanayake. Tree-connectivity: Evaluating the graphical structure of SLAM. In *Robotics and Automation (ICRA), 2016 IEEE International Conference on*, pages 1316–1322. IEEE, 2016.
- [18] Kasra Khosoussi, Gaurav S. Sukhatme, Shoudong Huang, and Gamini Dissanayake. Designing sparse reliable pose-graph SLAM: A graph-theoretic approach. *International Workshop on the Algorithmic Foundations of Robotics*, 2016.
- [19] Kasra Khosoussi, Matthew Giamou, Gaurav S Sukhatme, Shoudong Huang, Gamini Dissanayake, and Jonathan P How. Reliable graph topologies for SLAM. *International Journal of Robotics Research*, 2018. Accepted.
- [20] Andreas Krause and Daniel Golovin. Submodular function maximization. In Lucas Bordeaux, Youssef Hamadi, and Pushmeet Kohli, editors, *Tractability: Practical Approaches to Hard Problems*, pages 71–104. Cambridge University Press, 2014. ISBN 9781139177801.
- [21] Henrik Kretzschmar and Cyrill Stachniss. Information-theoretic compression of pose graphs for laser-based slam. *The International Journal of Robotics Research*, 31(11):1219–1230, 2012. doi: 10.1177/0278364912455072. URL <https://doi.org/10.1177/0278364912455072>.
- [22] Rainer Kümmerle, Giorgio Grisetti, Hauke Strasdat, Kurt Konolige, and Wolfram Burgard. g2o: A general framework for graph optimization. In *Robotics and Automation (ICRA), 2011 IEEE International Conference on*, pages 3607–3613. IEEE, 2011.
- [23] Spyridon Leonardos, Xiaowei Zhou, and Kostas Daniilidis. Distributed consistent data association via permutation synchronization. In *Robotics and Automation (ICRA), 2017 IEEE International Conference on*, pages 2645–2652. IEEE, 2017.
- [24] Jure Leskovec, Andreas Krause, Carlos Guestrin, Christos Faloutsos, Jeanne VanBriesen, and Natalie Glance. Cost-effective outbreak detection in networks. In *Proceedings of the 13th ACM SIGKDD international conference on Knowledge discovery and data mining*, pages 420–429. ACM, 2007.

- [25] J. Löfberg. Yalmip : A toolbox for modeling and optimization in matlab. In *In Proceedings of the CACSD Conference*, Taipei, Taiwan, 2004.
- [26] Michel Minoux. Accelerated greedy algorithms for maximizing submodular set functions. In *Optimization techniques*, pages 234–243. Springer, 1978.
- [27] Raúl Mur-Artal and Juan D. Tardós. ORB-SLAM2: an open-source SLAM system for monocular, stereo and RGB-D cameras. *IEEE Transactions on Robotics*, 33(5):1255–1262, 2017. doi: 10.1109/TRO.2017.2705103.
- [28] George L Nemhauser, Laurence A Wolsey, and Marshall L Fisher. An analysis of approximations for maximizing submodular set functions. *Mathematical Programming*, 14(1):265–294, 1978.
- [29] Esha D Nerurkar, Stergios I Roumeliotis, and Agostino Martinelli. Distributed maximum a posteriori estimation for multi-robot cooperative localization. In *Robotics and Automation, 2009. ICRA’09. IEEE International Conference on*, pages 1402–1409. IEEE, 2009.
- [30] Michael Otte and Nikolaus Correll. Any-com multi-robot path-planning with dynamic teams: Multi-robot coordination under communication constraints. In *Experimental Robotics*, pages 743–757. Springer, 2014.
- [31] Liam Paull, Guoquan Huang, Mae Seto, and John J Leonard. Communication-constrained multi-auv cooperative SLAM. In *Robotics and Automation (ICRA), 2015 IEEE International Conference on*, pages 509–516. IEEE, 2015.
- [32] Liam Paull, Guoquan Huang, and John J Leonard. A unified resource-constrained framework for graph SLAM. In *Robotics and Automation (ICRA), 2016 IEEE International Conference on*, pages 1346–1353. IEEE, 2016.
- [33] Friedrich Pukelsheim. *Optimal design of experiments*, volume 50. SIAM, 1993.
- [34] Sajad Saeedi, Michael Trentini, Mae Seto, and Howard Li. Multiple-robot simultaneous localization and mapping: A review. *Journal of Field Robotics*, 33(1):3–46, 2016.
- [35] Manohar Shamaiah, Siddhartha Banerjee, and Haris Vikalo. Greedy sensor selection: Leveraging submodularity. In *49th IEEE Conference on Decision and Control (CDC)*, pages 2572–2577. IEEE, 2010.
- [36] Maxim Sviridenko. A note on maximizing a submodular set function subject to a knapsack constraint. *Operations Research Letters*, 32(1):41–43, 2004.
- [37] Yulun Tian, Kasra Khosoussi, Matthew Giamou, Jonathan P. How, and Jonathan Kelly. Near-optimal budgeted data exchange for distributed loop closure detection. *arXiv*, 2018.
- [38] K. C. Toh, M.J. Todd, and R. H. Ttnc. SDPT3 – a matlab software package for semidefinite programming. *Optimization Methods and Software*, 11:545–581, 1999.
- [39] Lieven Vandenbergh, Stephen Boyd, and Shao-Po Wu. Determinant maximization with linear matrix inequality constraints. *SIAM journal on matrix analysis and applications*, 19(2):499–533, 1998.
- [40] Vijay V Vazirani. *Approximation algorithms*. Springer Science & Business Media, 2013.
- [41] J. Vial, H. Durrant-Whyte, and T. Bailey. Conservative sparsification for efficient and consistent approximate estimation. In *2011 IEEE/RSJ International Conference on Intelligent Robots and Systems*, pages 886–893, Sept 2011. doi: 10.1109/IROS.2011.6095128.